Published in final edited form as:
J Invest Dermatol. 2011 January ; 131(1): 177–187. doi:10.1038/jid.2010.290.

RXRα ablation in epidermal keratinocytes enhances UV radiation induced DNA damage, apoptosis, and proliferation of keratinocytes and melanocytes

Zhixing Wang[1], **Daniel J. Coleman**[1,2], **Gaurav Bajaj**[1], **Xiaobo Liang**[1], **Gitali Ganguli-Indra**[1], and **Arup Kumar Indra**[1,2,3,4,*]

[1] Department of Pharmaceutical Sciences, College of Pharmacy, Oregon State University, Corvallis, OR, 97331

[2] Molecular and Cellular Biology Program, Oregon State University, Corvallis, OR, 97331

[3] Environmental Health Sciences Center, Oregon State University, Corvallis, OR, 97331

[4] Department of Dermatology, Oregon Health & Science University, Portland, OR 97239, USA

Abstract

We show here that keratinocytic nuclear receptor Retinoid X Receptor α (RXRα) regulates mouse keratinocyte and melanocyte homeostasis following acute ultraviolet radiation (UVR). Keratinocytic RXRα has a protective role on UVR-induced keratinocyte and melanocyte proliferation/differentiation, oxidative stress mediated DNA damage and cellular apoptosis. We discovered that keratinocytic RXRα in a cell autonomous manner regulate mitogenic growth responses in skin epidermis via secretion of hbEGF, GMCSF, IL1-α and COX2, and activation of MAPK pathways. We identified altered expression of several keratinocyte-derived mitogenic paracrine growth factors such as ET-1, HGF, α–MSH, SCF and FGF2 in skin of mice lacking RXRα in epidermal keratinocytes (RXRα$^{ep-/-}$ mice), which in a non-cell autonomous manner modulated melanocyte proliferation and activation after UVR. RXRα$^{ep-/-}$ mouse represents a unique animal model where UVR induces melanocyte proliferation/activation in both epidermis and dermis. Considered together, our results suggest that RXR antagonists, together with inhibitors of cell proliferation can be effective to prevent solar UV radiation induced photo-carcinogenesis.

Keywords

RXRα; nuclear receptor; conditional somatic mutagenesis; epidermal homeostasis; keratinocytes; melanocytes; UV radiation; apoptosis; DNA damage; CPD; proliferation; autocrine; paracrine; mouse; transcription factor

INTRODUCTION

Skin is the largest organ in the body which prevents the organism from environmental physical and chemical traumas (Lippens et al., 2009). It is composed of the epidermis, and mesenchymal-derived dermis, which are separated by a basement membrane. The epidermis

*Correspondence: Tel: 541-737-5775(AI); Fax: 541-737-3999 (AI), Arup.Indra@oregonstate.edu.

CONFLICT OF INTEREST
The authors state no conflict of interest.

is mainly made up of keratinocytes, and composed of four layers: basal, spinous, granular and stratum corneum (Fuchs and Raghavan, 2002; Proksch et al., 2008). Melanocytes originate from neural crest cells (NCC), migrate to the basement membrane of human and mouse skin, and establish contact with keratinocytes (Fuchs and Raghavan, 2002; Proksch et al., 2008). Migration of melanocytes to the epidermis and hair follicles accounts for pigmentation in human (Haass and Herlyn, 2005; Hearing, 1999). In mouse neonatal skin, epidermal melanocytes are usually found during the early weeks after birth, whereas in adult skin, melanocytes are absent from epidermis and reside only in hair follicles and dermis (Hirobe, 1984, 2005; Quevedo and Fleischmann, 1980).

Unprotected ultraviolet radiation (UVR) is one of the major causes of skin cancer (Saraiya *et al.*, 2004; Strom and Yamamura, 1997). Epidemiological studies have suggested that childhood sunburn poses a significant risk of developing aggressive melanoma (Holman et al., 1983; Whiteman et al., 2001). UVB radiation (280–320 nm) can be absorbed by skin, causing sunburn, epidermal hyperplasia, skin aging, immune suppression and eventually skin cancer (Beissert and Schwarz, 1999; Bowden, 2004; Young, 1990). UVA (320–400 nm) is involved in skin carcinogenesis via indirect DNA damages, such as free radicals formation and oxidative reactions (Bickers and Athar, 2006; Yasui and Sakurai, 2000). Previous studies have demonstrated increased susceptibility of newborn, but not adult mice, is linked with melanoma in later life (Noonan et al., 2001; Hacker et al., 2005). Moreover, a single erythemal dose of ~900mJ/cm^2 (9 kJ/m^2) to 2- to 4-days old neonates was shown to be more effective than chronic treatments at inducing melanoma in mice models (Noonan et al., 2001; Hacker et al., 2005; Hacker et al., 2006).

The first step of UV-induced skin carcinogenesis is causing DNA damage in the skin, which mainly includes cyclobutane pyrimidine dimers (CPD) and pyrimidine (6-4) pyrimidone photoproducts (6-4 PP) (Friedberg, 2003; Mitchell and Nairn, 1989; Setlow et al., 1963). Moreover, UVR increases oxidative stress-induced formation of 8-hydroxy-2′-deoxyguanosine (8-oxo-dG), which is also linked to skin carcinogenesis (Hattori et al., 1996; Kunisada et al., 2005; Wilgus et al., 2002; Wulff et al., 2008). The next steps include cell cycle arrest, DNA repair, immunosuppression, gene mutation and transformation (D'Errico *et al.*, 2007; de Gruijl, 2008; Olivier *et al.*, 2004; Ouhtit *et al.*, 2000). In general, keratinocytes give rise to daughter cells that terminally differentiate; however, if the DNA damage cannot be repaired during the period of cell cycle arrest, keratinocytes are prone to die via apoptosis (Eckert et al., 2002). p53 is induced in both keratinocytes and fibroblasts after UVB irradiation, and has a unique role in inducing apoptotic pathways (D'Errico et al., 2007; Donehower and Lozano, 2009). UVR also stimulates expression of keratinocyte-derived autocrine factors, such as Cyclooxygenase-2 (COX2), Granulocyte-macrophage colony-stimulating factor (GMCSF), and interleukins in mouse skin (Hirobe et al., 2004a; Rundhaug et al., 2007). Paracrine factors, such as endothelins and pro-opiomelanocortin (POMC), which are secreted by keratinocytes and regulate melanocyte proliferation, have been implicated to be altered by UVR exposure (Chakraborty et al., 1996; Imokawa et al., 1992; Kadekaro and Abdel-Malek, 2007).

Retinoids have been shown to regulate skin development, differentiation and homeostasis, which are mediated by nuclear receptors (NRs) such as retinoid acid receptors (RARs) and retinoid-X-receptors (RXRs) (Chambon, 1993, 1996). RXRα, the most abundant isoform of RXR in skin, is a central transcriptional regulator in modulating gene expression by heterodimerization with other NRs (Li et al., 2001). RXRα is expressed in both mouse and human epidermis, and RXRα null mice are embryonic lethal between E13.5 and E16.5 (Kastner et al., 1994; Sucov et al., 1994). Using Cre-loxP strategy, we were able to obtain RXRα$^{ep-/-}$ mice which selectively lacked RXRα in epidermal keratinocytes (Li et al., 2000; Metzger et al., 2003).

Previous studies have reported that RXRα ablation in skin caused alopecia and altered homeostasis of proliferation/differentiation of epidermal keratinocytes (Li et al., 2001). RXRα also has a protective role in DMBA/TPA induced formation of epidermal and melanocytic tumors (Indra et al., 2007; Hyter et al., 2010). In order to investigate the possible role of keratinocytic RXRα in UV-induced skin damage, we subjected RXRα$^{ep-/-}$ and control (CT) RXRα$^{L2/L2}$ neonatal mice to an acute UVR to study keratinocytes and melanocytes homeostasis. UVR caused increased apoptosis, proliferation and differentiation in keratinocytes of RXRα$^{ep-/-}$ compared to CT mice. UVR also enhanced oxidative stress-induced DNA damage in melanocytes, as well as increased melanocyte proliferation in both epidermis and dermis of RXRα$^{ep-/-}$ mice. Our data indicated a critical role of keratinocytic RXRα in maintaining skin homeostasis after UV exposure.

RESULTS

UVR enhances formation of DNA adducts in RXRα$^{ep-/-}$ mice

In order to evaluate DNA damage level after UVR, dorsal skin of CT and RXRα$^{ep-/-}$ neonatal mice was exposed to a single dose of UVR (UVA and UVB), and harvested after 24, 48 and 72 hours (see Materials and Methods). Without UV treatment, very few thymine dimers were observed in CT and RXRα$^{ep-/-}$ mice epidermis. At 24 and 48 hours after UV exposure, the number of thymine dimer positive cells in keratinocytes and melanocytes significantly increased, then dropped at 72 hours (Figure 1a and S1). However, CPD formation in epidermis was not influenced by RXRα ablation (Figure 1a and data not shown). Similarly, oxidative stress-induced DNA damage in both epidermis and dermis was determined by immunohistochemistry (IHC) using anti-8-oxo-dG and anti-TRP2 antibodies. At 48 hours after UV exposure, 8-oxo-dG positive cells were significantly increased in both control and mutant mice, and their numbers dropped at 72 hours. Most of the oxidative DNA damage occurred in dermal melanocytes, and ~2 fold more positive cells were found in RXRα$^{ep-/-}$ mice compared to CT mice (Figure 1b). Above results suggest that RXRα has a protective effect on oxidative stress-induced DNA damage in mouse skin.

Increased apoptosis in RXRα$^{ep-/-}$ mice after UV irradiation

Terminal deoxynucleotidyl transferase-mediated dUTP nick end labeling (TUNEL) assays are used to detect DNA strand breaks, which is often associated with apoptosis (DeCoster, 2003; Lu et al., 1999; Matsumura et al., 2004; Ouhtit et al., 2000). The percentage of epidermal TUNEL positive cells in RXRα$^{ep-/-}$ mice was 3 and 2 fold higher at 24 and 72 hours, respectively, compared to the controls (Figure 1c and d). At 48 hours, although percentage of TUNEL positive cells was similar in epidermis, the apoptosis rate was higher in RXRα$^{ep-/-}$ mice compared to CT mice in the dermis, indicating a protective role of keratinocytic RXRα in reducing strand breaks formation in dermal compartment (Figure 1c). Similar results were obtained by IHC study using an antibody against caspase 3 which is a mediator of the execution phase in apoptosis [(data not shown) Cohen, 1997]. No difference in apoptosis was observed between non-irradiated CT and RXRα$^{ep-/-}$ mice at all timepoints (see Figure S3a). Together, the above results suggest that keratinocytic RXRα plays a role in regulating apoptosis in both epidermis and dermis.

RXRα$^{ep-/-}$ mice exhibited altered epidermal proliferation and differentiation after UV irradiation

Histological analysis of hemotoxylin & eosin (H&E) stained skin sections revealed presence of significant epidermal hyperplasia in RXRα$^{ep-/-}$ mice compared to CT mice 48 and 72 hours after UVR (Figure 2a). To determine the changes in keratinocyte proliferation of RXRα$^{ep-/-}$ mice, IHC analyses were performed for proliferation markers Ki67 and cytokeratin 14 (K14) (see Fig. 2b and Figure S4a). Epidermal Ki67 positive cell number was

2 fold higher in RXRα$^{ep-/-}$ mice, 24 and 48 hours after acute UV exposure, respectively (see Fig. 2b and d). Similarly, western blot analyses revealed that expression of K14 peaked 48 hours after UVR and was higher in the mutant skin compared the CT skin before and 24, 72 hours after UV radiation (Figure 2e). No significant difference in percent Ki67 positive cells was found between non-irradiated CT and RXRα$^{ep-/-}$ mice skin at all timepoints (Figure S3b). The expression levels of early [Keratin 10 (K10)] and late (Filaggrin and Loricrin) differentiation markers were induced after UV radiation in both CT and RXRα$^{ep-/-}$ skin, and were higher in mutants compared to CT skin at all timepoints (24, 48 and 72 hours) after UV irradiation (Figure S4b–d). These studies indicate that keratinocytic RXRα has a protective role in skin keratinocytes after UV irradiation, and selective ablation of RXRα in epidermal keratinocytes leads to increased keratinocyte proliferation and differentiation.

Ablation of RXRα in epidermis increased expression of keratinocyte derived autocrine factors

In order to determine whether altered keratinocyte proliferation and differentiation in mutant skin is due to impaired mitogenic responses, real-time qPCR analyses were performed for diffusible growth factors such as heparin-binding EGF-like growth factor (hbEGF) and GMCSF on RNA isolated from control and mutant (Braunstein et al., 1994; Werner and Smola, 2001; Yoshida et al., 2008). Expressions of both factors were upregulated by 2 fold in skin of RXRα$^{ep-/-}$ compared to CT mice and had highest expression level 24 hours after UVR (Figure 3a). Relative expression of interleukin-1α (IL-1α), a major pro-inflammatory cytokine was modestly increased in the mutant mice before and 24 hours after UVR (see Fig. 3b). Similarly, relative expression level of COX2, which plays an important role in inflammation, was significantly higher in the mutant skin 24 hours after UV treatment (see Fig. 3b). Expression of all these genes dropped 72 hours after UV except for COX2. These results demonstrated that keratinocytic RXRα, in a cell autonomous manner, modulates keratinocyte proliferation and/or differentiation via secretion of mitogenic growth factors and cytokines within a short time window after UVR.

Altered mitogenic and apoptotic responses in the skin of RXRα$^{ep-/-}$ mice after UVR

We hypothesized that increased proliferation, differentiation and altered apoptotis in RXRα$^{ep-/-}$ mice may be due to alteration of mitogenic and apoptotic signaling following UV irradiation. To test that, western blot analyses were performed for determining the protein levels and phosphorylation status of key MAPK proteins (ERK and JNK), and the expression level of transcription factor p53 in CT and RXRα$^{ep-/-}$ (MT) mice skin (see Fig. 3e) (Eckert et al., 2002;Kulesz-Martin et al., 2005). The expression level of both ERK and JNK was similar between control and mutant skin at 0 and 24 hours timepoints, and modestly higher in mutant at 72 hours. Interestingly, the protein levels of phospho ERK and phospho JNK were slightly lower at 24 hours, but higher at 72 hours in mutant, compared to the CT skin (Figure 3e). Expression of tumor suppressor p53 and its direct target p21 was similarly induced in both control and mutant skin after UVR. Induction of both p53 and p21 peaked after 24 hours of UVR in CT mice. However, in mutant mice skin, these induction levels peaked 72 hours after UV irradiation, suggesting delayed p53-mediated cellular responses in RXRα$^{ep-/-}$ mice. Above results suggest that enhanced proliferation, differentiation and increased apoptosis in the mutant skin can be due to aberrant growth promoting mitogenic and altered apoptotic responses in those mice following UV irradiation.

Keratinocytic RXRα is involved in keratinocyte-melanocyte cross-talk

It is possible that ablation of RXRα in epidermal keratinocytes impacts melanocyte homeostasis. We therefore performed double staining with antibodies against proliferation

marker PCNA and melanocyte specific marker TRP1 on control and mutant mice skin. Without UVR, only a few melanocytes were identified in CT and RXRα$^{ep-/-}$ mice epidermis 2 days postnatal (P2) (Figure 4a, left panel and Figure 4c). 48 hours after UVR, the number of epidermal melanocytes in CT mice increased ~2 fold (~2 per field) compared to non-irradiated skin. In contrast, epidermal melanocytes in mutant are significantly higher compared to CT (~3 per field) at 48 hours. 72 hours after UVR, epidermal melanocyte number peaked for both control (~4 per field), and mutant (~4.5 per field) (Figure 4a and c). We also performed Fontana-Masson staining to detect pigmented melanocytes in CT and RXRα$^{ep-/-}$ skin at all timepoints (Figure 4b and data not shown). Comparable amount of melanocytes were found in the dermis of control and mutant mice before and 24 hours after UVR (Figure 4b). At 24 hours, large clusters of pigmented melanocytes were found in the dermis (Figure 4b, middle panel). Interestingly, 48 hours after UVR, RXRα$^{ep-/-}$ mice skin exhibited a ~2 fold higher number of pigmented melanocytes in the dermal compartment compared to CT (Figure 4b, right panel, and Fig. 4d). Consistently, increased TRP2 positive melanocytes were detected in the dermis of mutant skin 48 hours after UVR (see Fig.1b, data not shown). Above results suggest that RXRα$^{ep-/-}$ mice are more sensitive to UVR-induced melanocyte activation/proliferation in both epidermis and dermis.

In order to confirm the *ex vivo* data, primary melanocytes were cultured in keratinocyte-derived conditioned medium from CT and mutant mice. Melanocyte growth medium was used as control. Murine melanocytes showed an increased growth 24 hours after incubation with keratinocyte conditioned medium from control or mutant mice compared to its own medium (see Fig. 4e). Melanocytes cultured 24 hours in keratinocyte-derived conditioned medium from RXRα$^{ep-/-}$ mice skin after UVR had higher proliferation than those cultured in conditioned medium from CT skin (Figure 4e).

To determine the mechanism(s) of keratinocytic RXRα modulated melanocyte proliferation, we studied the relative mRNA expression level of paracrine factors such as endothelin 1 (ET-1), fibroblast growth factor-2 (FGF2), stem cell factor (SCF) and POMC, which are secreted by keratinocytes to stimulate melanocyte proliferation (Figure 4c and d) (Chakraborty et al., 1996; Haass and Herlyn, 2005; Imokawa et al., 1992; Slominski and Paus, 1993; Yada et al., 1991). Relative mRNA expression levels of ET-1, FGF2 and SCF were more than 2 fold higher in mutant skin before and 24 hours after UV irradiation (Fig. 3c and d). Overall, our results provide compelling evidence that keratinocytic RXRα, in cooperation with UVR, regulate melanocyte homeostasis by repressing secretion of paracrine mitogenic growth factors.

DISCUSSION

We have identified RXRα as a key regulator of UVR-induced cellular responses. Ablation of RXRα in neonatal mouse epidermis causes skin hyperplasia, which is reflected by increased epidermal proliferation and differentiation. RXRα also regulated oxidative stress induced DNA damage and skin apoptosis in cell-autonomous and non-cell autonomous manner. Moreover, epidermal RXRα was found to be involved in suppressing activation and/or proliferation of epidermal and dermal melanocytes after acute UV irradiation, mainly by controlling the keratinocyte-melanocyte cross-talk through secretion of paracrine factors.

Keratinocytic RXRα protects melanocytes from oxidative stress induced DNA damage after UVR

We have found that CPD formation in keratinocytes initiates early after UVR and lasts for at least 2 days. In contrast, CPD formation in melanocyte were observed around 48 hours after UVR and decreased soon afterwards, indicating a possible different mechanism of DNA repair in melanocytes from keratinocytes. Similar results of UVR induced CPD formation in

murine keratinocytes and melanocytes were reported earlier (Walker et al., 2009). Present study has shown that dermal melanocytes in the skin of mutant mice were more susceptible to oxidative stress induced DNA damage as confirmed by increased positive staining for 8-oxo-dG (Figure. 1b), the mechanism of which needs to be better understood. In human melanocytes, UV induces reactive oxygen species (ROS) which causes 8-oxo-dG signature mutation after UVR (Charron et al., 2000; Jin et al., 2007).

Paracrine factor α-MSH has been shown to protect human melanocytes against UV-induced oxidative stress (Song et al., 2009). Here we observed an increased expression of POMC (precursor of α-MSH), and also an increase in oxidative stress in the mutant skin, suggesting an alternative mechanism of keratinocytic RXRα-mediated protection of melanocytes against ROS-induced oxidative stress after UVR. To our knowledge, these results are previously unreported. The difference between previous *in vitro* study and our *ex vivo* study can be attributed to (a) the inherent differences between human and mouse melanocytes, (b) epidermal versus dermal origin of melanocytes in the two studies, and/or (c) complex micro-environmental effects in *ex vivo* study compared to *in vitro* study. Overall, these results demonstrate that keratinocytic RXRα, in a non-cell autonomous manner, protects melanocytes and other dermal cells from oxidative stress induced DNA damage following solar UV irradiation.

Altered UVR-induced apoptotic responses in mutant skin

In neonatal mice skin, we have observed that epidermal keratinocyte apoptosis significantly increased and peaked at 24 hours post UVR, which then dropped around 72 hours, thereby corroborating previous results reported earlier in adult mice by Ouhtit et al., (2000). Percent apoptotic cells were higher in RXRα$^{ep-/-}$ skin than in CT mice at all timepoints after UV exposure, suggesting a higher penetration of UVR through epidermal barrier to dermis in RXRα$^{ep-/-}$ mice. The increased UVR-induced apoptosis in the mutant skin can be attributed to additional DNA damage besides thymine dimer formation, impaired DNA repair mechanism and/or altered apoptotic responses.

UVB induces p53 expression in wildtype adult mouse skin with a maximum level at 24 hours after single dose of UVR (Campbell et al., 1993; Matsumura et al., 2004). Our western blot analysis and p53 IHC staining confirmed that RXRα ablation in epidermis delayed the induction of p53, and in turn, its target gene p21 expression beyond 24 hours, which didn't explain the increased apoptosis in RXRα$^{ep-/-}$ mice 24 hours after UV exposure (Figure 3 and S2). Those results suggest that increased apoptotic responses in RXRα$^{ep-/-}$ mice may be mediated by both p53-dependent and independent pathways.

Keratinocytic RXRα regulates UVR-induced melanocyte proliferation/activation via secretion of paracrine factors

Melanocytes were shown to respond to UVB exposure and exhibited an increase in proliferation in both human and mouse skin compared with no treatment groups (Sato and Kawada, 1972; Stierner et al., 1989; van Schanke et al., 2005; Walker et al., 2009). Our data of TRP1 staining on neonatal CT and mutant mice confirmed that epidermal melanocyte numbers peaked 3 days after UVR, which corroborated well with an earlier report (Walker et al., 2009). However, in RXRα$^{ep-/-}$ mice, epidermal and dermal melanocyte numbers were always higher after UVR, suggesting a rapid response to UV effects in those mice, which may be due to increased sensitivity and susceptibility of RXRα$^{ep-/-}$ mice to UVR (see Fig. 4a, c and d). Our *in vitro* proliferation assay showed a significant increase in melanocyte number after culture with conditioned keratinocyte medium (KM) from RXRα$^{ep-/-}$ mice, compared to the control conditioned medium following UV exposure, indicating an enhanced secretion of growth-promoting mitogenic paracrine factors from

mutant keratinocytes. RT-qPCR studies also confirmed increased expression of several mitogenic paracrine factors such as ET-1, POMC, SCF and FGF2 in the mutant skin, all of which have been reported to regulate melanocyte proliferation and melanogenesis (Chakraborty et al., 1996; Imokawa et al., 1992; Slominski and Paus, 1993; Yada et al., 1991). Recent studies suggested that p53 promotes melanogenic cytokine POMC expression, as well as ET-1 and SCF production in epidermal hyperpigmented keratinocytes induced by UVR (Cui et al., 2007; Murase et al., 2009). Choromatin immunoprecipitation (ChIP) assay on mouse skin extracts showed no direct recruitment of RXRα on p53 promoter (Hyter et al., 2010). Therefore, the mechanism of deregulated p53 expression in the mutant mice following UV exposure is currently unknown. These results suggest a multiple levels of gene regulation and confirm that RXRα can directly or indirectly modulate expression of genes encoding paracrine factors involved in modulating melanocyte homeostasis.

We have found RXRα as a modulator of skin keratinocyte and melanocyte homeostasis via autocrine and paracrine signaling. Generation of bigenic mice with selective deletion of both RXRα and each one of the paracrine factors will help us reveal the non-cell autonomous effects mediated by RXRα. RXRα heterodimeric partners that are involved in mediating those UVR-induced cellular responses also need to be identified. Our research is expected to help generate mouse models for studying UV-induced photocarcinogenesis and melanomagenesis, and develop efficient strategies to prevent and/or cure UV-induced squamous carcinoma and melanoma.

MATERIALS AND METHODS

Mice

Mice carrying LoxP-site-containing (floxed) $RXR\alpha^{L2}$ alleles were bred with hemizygous $K14\text{-}Cre^{(tg/0)}$ transgenic mice, to produce $K14\text{-}Cre^{(tg/0)}/RXR\alpha^{L2/L2}$ mice (Li et al., 2000; Metzger et al., 2003). The constitutively active K14-Cre transgene selectively delete the gene encoding RXRα in epidermis to generate $RXR\alpha^{ep-/-}$ mice, and $RXR\alpha^{L2/L2}$ mice were used as control (Metzger et al., 2003). RXRα ablation in the epidermis was verified by PCR analyses of DNA isolated from tail biopsies as described (Li et al., 2000). All CT and $RXR\alpha^{ep-/-}$ mice were on similar C57BL/6J (~70%), SV129 (~20%) and SJL (~10%) mixed genetic background. 8 to 10 mice combined from multiple litters were used in each group at each timepoint. CT and MT littermates were selected in each group and for all timepoints in order to minimize variability due to the mixed background. OSU IACUC approval was obtained for animal experiments.

UV radiation

2 day old mice (P2) were exposed to a single dose of $900mJ/cm^2$ UV light from a bank of four Philips FS-40 UV sunlamps. Besides the majority of UVB output, there was also some output of UVA spectrum. The irradiance of the sunlamps was measured with an IL-1400A radiometer with a SEE240 UVB detector (International Light, Newburyport, MA).

Isolation of Skin Samples

Mice were euthanized 24, 48 and 72 hrs after UV irradiation, and skin samples were retrieved. Mice for 0 hour time point were taken 1 day after birth without UV treatment. For each mouse, three pieces of $0.5cm^2$ size skin biopsies were taken for immunohistochemistry, RNA and protein isolation, respectively.

Histological analysis

Skin biopsies were fixed in 4% paraformaldehyde overnight, embedded in paraffin blocks, and 5 μm paraffin sections were sectioned using Leica RM2255 microtome. Hematoxylin and Eosin staining was performed as described (Indra et al., 2005a; Indra et al., 2005b). Fontana-Masson Staining was performed using a commercial kit according to the manufacturer's protocol (American MasterTech, Lodi, CA).

Immunohistochemistry

5 μm paraffin sections were deparaffinized, rinsed with water and antigen retrieval was performed with pH 6.0 citrate buffer at 95°–100°C for 20 minutes. Slides were washed with PBS (x3), blocked with 10% Normal Goat Serum (Vector Laboratories, CA) for 30 minutes. Then slides were incubated overnight with primary antibodies (see supplementary methods), followed by three washes with PBS + 0.05% Tween20 and incubated with fluorescently labeled secondary antibody for an hour at room temperature. Nuclei were visualized with DAPI. After the final washes, slides were dehydrated through series of ethanol washes, cleared in xylene and mounted with DPX mounting media. All images were captured at 40x magnification using Carl Zeiss Axio Imager Z1 fluorescent microscope and AxioCam camera. Data was analyzed and quantified using Adobe Photoshop and Image J software. Multiple IHC fields on each slide from control and mutant mice skin were randomly chosen and 10–15 such fields/slide were counted. The slides were analyzed double-blinded by two observers independently. All experiments in each category were repeated at least 3 times and the results obtained were very consistent between various experiments.

Preparation of Keratinocyte-Conditioned Medium

Dorsal skin from taken neonatal mice was incubated overnight in CnT-07 medium (CELLnTEC, Bern, Switzerland) containing 5mg/mL dispase (Gibco, NY) and 5X Antibiotic/Antimycotic Solution (CellnTEC) at 4°C to dissociate epidermis. Keratinocytes were dissociated from epidermis by incubating in TrypLE Select (Gibco). Cells were collected by centrifugation (160xg) and seeded into uncoated 100mm dishes at a density of 5.0×10^4 cells/cm^2. Cells were cultured in CnT-07 containing 1X Antibiotic/Antimycotic at 35°C, 5% CO_2. Growth medium was changed on Day 2 of culture. 48 hours after medium change, medium was either removed or stored at −20°C until use, or culture dishes containing cells were irradiated with 850mJ/cm^2 UV. Irradiated cells were placed back at 35°C, 5% CO_2 for 24 hours, after which, medium was collected and stored at −20°C until use.

Melanocyte Proliferation Assay

Primary murine melanocytes were obtained from Yale University (New Haven, CT). Cells were maintained in melanocyte growth medium, consisting of OPTI-MEM (Invitrogen, Carlsbad, CA) containing 7% Heat-Inactivated Horse Serum (Invitrogen, Carlsbad, CA), 10ng/mL TPA, and 1X Antibiotic/Antimycotic (CELLnTEC). Growth conditions were 37°C, 5% CO_2. Cells were harvested using TrypLE Select (Gibco) and seeded into 96-well White/Clear plate (BD Biocoat, San Jose, California) at a density of 5×10^3 cells/well. Cells were placed under normal growth conditions for 3 hours to allow for complete adherence to plate. Melanocyte growth medium was removed, and cells were placed under starvation conditions overnight using basal Dulbecco's Modified Eagles Medium (DMEM) containing 1X Antibiotic/Antimycotic. Starvation medium was then removed and replaced with a 1:1 mixture of keratinocyte-conditioned medium (either UV or non-UV treated, $RXR\alpha^{ep-/-}$ or $RXR\alpha^{L2/L2}$ conditioned) and melanocyte growth medium. Unmixed melanocyte growth medium was used as control. Cells were incubated for 24 hours at 37°C, 5% CO_2, after which medium was removed, and cell number assayed for using a CyQUANT NF Cell

Proliferation Assay Kit (Invitrogen) according to the manufacturer's recommendation. All assays were performed in triplicate.

RT-qPCR

RNA extraction and cDNA preparation were performed as described (Indra et al., 2005b). Real-time PCR was performed on an ABI 7500 Real-Time PCR system using SYBR green methodology (Indra et al., 2005a; Indra et al., 2005b). Relative gene expression analysis of the RT-qPCR data was performed using HPRT as an internal control. Our RT-qPCR results using multiple primers from different exons of HPRT confirmed that its expression did not change as a result of RXRa ablation compared to other controls such as GAPDH or β-actin. Primer sequences used are shown in Table S1. All assays were performed in triplicates.

Western Blotting

Both control and RXRα$^{ep-/-}$ mice were exposed to UV irradiation with a single dose (900 mJ/cm^2) and the skin biopsies were collected at 0, 24 and 72 hours after exposure. Skin samples were homogenized, and proteins were extracted with a lysis buffer (150mM NaCl, 50mM Tris pH 7.5, 5mM EDTA, and 1% Nonidet P-40, 0.1% SDS, 0.5% sodium deoxycholate) containing protease inhibitors (2μg/ml Aprotinin, 2μg/ml Leupeptin, 100μg/ml Pefabloc and 1μg/ml Pepstatin). Equal amounts of protein extract (25 μg) from each lysate were resolved using SDS polyacrylamide-gel electrophoresis and transferred onto a nitrocellulose membrane. Blots were blocked overnight with 5% nonfat dry milk and incubated with specific antibodies (supplementary methods). All western blot experiments were done in triplicates, using a minimum of three biological replicates from each group of mice.

Statistical Analysis—Statistical significance of differences between groups was assessed using Graphpad Prism software by two-tailed unpaired t-test and Bonferroni-Step down (Holm) analysis. Quantification of TUNEL or Ki67 positive cells of CT and MT mice was determined by counting total number of TUNEL or Ki67 positive cells, and expressed as a percentage of DAPI$^+$ cells. Similarly, number of epidermal and dermal melanocytes was counted in multiple skin section and expressed as melanocytes per field. IHC data was quantified using Adobe Photoshop and Image J software, and epidermal thickness was quantified using Leica One-Suite software. Multiple sections were analyzed from 8–10 mice of each genotype and for each timepoint, and significance was determined using a student's unpaired t-test. Data obtained from each group of control and mutant mice for each time point were combined for calculating the mean data and SEM. Sensitivity analysis with mixed models showed that the litter effects are not significant and simple model with the subset is justified. All statistical analyses were independently performed double-blinded by two investigators.

Supplementary Material

Refer to Web version on PubMed Central for supplementary material.

Acknowledgments

We would like to thank Prof. Pierre Chambon and Daniel Metzger for helpful advice and critically reviewing the manuscript, Cliff Pereira for statistical analysis. We would also like to thank Talicia Savage, Erin Bredeweg and Steven Ma for help in sample processing. These studies were supported by grant ES016629-01A1 (AI) from NIEHS at National Institutes of Health, an OHSU Medical Research Foundation grant to AI, and by a NIEHS Center grant (ES00210) to the Oregon State University Environmental Health Sciences Center. We also thank Drs. Wayne Kradjan and Gary DeLander of the OSU College of Pharmacy for continuous support and encouragement.

References

Beissert S, Schwarz T. Mechanisms involved in ultraviolet light-induced immunosuppression. J Investig Dermatol Symp Proc. 1999; 4:61–4.

Bickers DR, Athar M. Oxidative stress in the pathogenesis of skin disease. J Invest Dermatol. 2006; 126:2565–75. [PubMed: 17108903]

Bowden GT. Prevention of non-melanoma skin cancer by targeting ultraviolet-Blight signalling. Nat Rev Cancer. 2004; 4:23–35. [PubMed: 14681688]

Braunstein S, Kaplan G, Gottlieb AB, Schwartz M, Walsh G, Abalos RM, et al. GM-CSF activates regenerative epidermal growth and stimulates keratinocyte proliferation in human skin in vivo. J Invest Dermatol. 1994; 103:601–4. [PubMed: 7930689]

Campbell C, Quinn AG, Angus B, Farr PM, Rees JL. Wavelength specific patterns of p53 induction in human skin following exposure to UV radiation. Cancer Res. 1993; 53:2697–9. [PubMed: 8504406]

Chakraborty AK, Funasaka Y, Slominski A, Ermak G, Hwang J, Pawelek JM, et al. Production and release of proopiomelanocortin (POMC) derived peptides by human melanocytes and keratinocytes in culture: regulation by ultraviolet B. Biochim Biophys Acta. 1996; 1313:130–8. [PubMed: 8781560]

Chambon P. The molecular and genetic dissection of the retinoid signalling pathway. Gene. 1993; 135:223–8. [PubMed: 8276261]

Chambon P. A decade of molecular biology of retinoic acid receptors. Faseb J. 1996; 10:940–54. [PubMed: 8801176]

Charron RA, Fenwick JC, Lean DR, Moon TW. Ultraviolet-B radiation effects on antioxidant status and survival in the zebrafish, Brachydanio rerio. Photochem Photobiol. 2000; 72:327–33. [PubMed: 10989602]

Cohen GM. Caspases: the executioners of apoptosis. Biochem J. 1997; 326 (Pt 1):1–16. [PubMed: 9337844]

Cui R, Widlund HR, Feige E, Lin JY, Wilensky DL, Igras VE, et al. Central role of p53 in the suntan response and pathologic hyperpigmentation. Cell. 2007; 128:853–64. [PubMed: 17350573]

D'Errico M, Lemma T, Calcagnile A, Proietti De Santis L, Dogliotti E. Cell type and DNA damage specific response of human skin cells to environmental agents. Mutat Res. 2007; 614:37–47. [PubMed: 16879839]

de Gruijl FR. UV-induced immunosuppression in the balance. Photochem Photobiol. 2008; 84:2–9. [PubMed: 18173695]

DeCoster MA. Group III secreted phospholipase A2 causes apoptosis in rat primary cortical neuronal cultures. Brain Res. 2003; 988:20–8. [PubMed: 14519523]

Donehower LA, Lozano G. 20 years studying p53 functions in genetically engineered mice. Nat Rev Cancer. 2009; 9:831–41. [PubMed: 19776746]

Eckert RL, Efimova T, Dashti SR, Balasubramanian S, Deucher A, Crish JF, et al. Keratinocyte survival, differentiation, and death: many roads lead to mitogen-activated protein kinase. J Investig Dermatol Symp Proc. 2002; 7:36–40.

Friedberg EC. DNA damage and repair. Nature. 2003; 421:436–40. [PubMed: 12540918]

Fuchs E, Raghavan S. Getting under the skin of epidermal morphogenesis. Nat Rev Genet. 2002; 3:199–209. [PubMed: 11972157]

Haass NK, Herlyn M. Normal human melanocyte homeostasis as a paradigm for understanding melanoma. J Investig Dermatol Symp Proc. 2005; 10:153–63.

Hacker E, Irwin N, Muller HK, Powell MB, Kay G, Hayward N, et al. Neonatal Ultraviolet Radiation Exposure Is Critical for Malignant Melanoma Induction in Pigmented Tpras Transgenic Mice. J Investig Dermatol. 2005; 125(5):1074–1077. [PubMed: 16297212]

Hacker E, Muller HK, Irwin N, Gabrielli B, Lincoln D, Pavey S, et al. Spontaneous and UV radiation-induced multiple metastatic melanomas in Cdk4R24C/R24C/TPras mice. Cancer Res. 2006; 66(6): 2946–2952. [PubMed: 16540642]

Hattori Y, Nishigori C, Tanaka T, Uchida K, Nikaido O, Osawa T, et al. 8-hydroxy-2′-deoxyguanosine is increased in epidermal cells of hairless mice after chronic ultraviolet B exposure. J Invest Dermatol. 1996; 107:733–7. [PubMed: 8875958]

Hearing VJ. Biochemical control of melanogenesis and melanosomal organization. J Investig Dermatol Symp Proc. 1999; 4:24–8.

Hirobe T. Histochemical survey of the distribution of the epidermal melanoblasts and melanocytes in the mouse during fetal and postnatal periods. Anat Rec. 1984; 208:589–94. [PubMed: 6731864]

Hirobe T. Role of keratinocyte-derived factors involved in regulating the proliferation and differentiation of mammalian epidermal melanocytes. Pigment Cell Res. 2005; 18:2–12. [PubMed: 15649147]

Hirobe T, Furuya R, Hara E, Horii I, Tsunenaga M, Ifuku O. Granulocyte-macrophage colony-stimulating factor (GM-CSF) controls the proliferation and differentiation of mouse epidermal melanocytes from pigmented spots induced by ultraviolet radiation B. Pigment Cell Res. 2004a; 17:230–40. [PubMed: 15140068]

Hirobe T, Furuya R, Ifuku O, Osawa M, Nishikawa S. Granulocyte-macrophage colony-stimulating factor is a keratinocyte-derived factor involved in regulating the proliferation and differentiation of neonatal mouse epidermal melanocytes in culture. Exp Cell Res. 2004b; 297:593–606. [PubMed: 15212959]

Holman CD, Armstrong BK, Heenan PJ. A theory of the etiology and pathogenesis of human cutaneous malignant melanoma. J Natl Cancer Inst. 1983; 71:651–656. [PubMed: 6578359]

Hyter S, Bajaj G, Liang X, Barbacid M, Ganguli-Indra G, Indra AK. Loss of nuclear receptor RXRalpha in epidermal keratinocytes promotes the formation of Cdk4-activated invasive melanomas [Internet]. Pigment Cell Melanoma Res. 2010 Jun 15. [Epub ahead of print].

Imokawa G, Yada Y, Miyagishi M. Endothelins secreted from human keratinocytes are intrinsic mitogens for human melanocytes. J Biol Chem. 1992; 267:24675–80. [PubMed: 1280264]

Indra AK, Castaneda E, Antal MC, Jiang M, Messaddeq N, Meng X, et al. Malignant transformation of DMBA/TPA-induced papillomas and nevi in the skin of mice selectively lacking retinoid-X-receptor alpha in epidermal keratinocytes. J Invest Dermatol. 2007; 127:1250–60. [PubMed: 17301838]

Indra AK, Dupe V, Bornert JM, Messaddeq N, Yaniv M, Mark M, et al. Temporally controlled targeted somatic mutagenesis in embryonic surface ectoderm and fetal epidermal keratinocytes unveils two distinct developmental functions of BRG1 in limb morphogenesis and skin barrier formation. Development. 2005a; 132:4533–44. [PubMed: 16192310]

Indra AK, Mohan WS 2nd, Frontini M, Scheer E, Messaddeq N, Metzger D, et al. TAF10 is required for the establishment of skin barrier function in foetal, but not in adult mouse epidermis. Dev Biol. 2005b; 285:28–37. [PubMed: 16039642]

Jin GH, Liu Y, Jin SZ, Liu XD, Liu SZ. UVB induced oxidative stress in human keratinocytes and protective effect of antioxidant agents. Radiat Environ Biophys. 2007; 46:61–8. [PubMed: 17279358]

Kadekaro AL, Abdel-Malek ZA. Walking in the footsteps of giants: melanocortins and human pigmentation, a historical perspective. Pigment Cell Res. 2007; 20:150–2. [PubMed: 17516922]

Kastner P, Grondona JM, Mark M, Gansmuller A, LeMeur M, Decimo D, et al. Genetic analysis of RXR alpha developmental function: convergence of RXR and RAR signaling pathways in heart and eye morphogenesis. Cell. 1994; 78:987–1003. [PubMed: 7923367]

Kulesz-Martin M, Lagowski J, Fei S, Pelz C, Sears R, Powell MB, et al. Melanocyte and keratinocyte carcinogenesis: p53 family protein activities and intersecting mRNA expression profiles. J Investig Dermatol Symp Proc. 2005; 10:142–52.

Kunisada M, Sakumi K, Tominaga Y, Budiyanto A, Ueda M, Ichihashi M, et al. 8-Oxoguanine formation induced by chronic UVB exposure makes Ogg1 knockout mice susceptible to skin carcinogenesis. Cancer Res. 2005; 65:6006–10. [PubMed: 16024598]

Li M, Chiba H, Warot X, Messaddeq N, Gerard C, Chambon P, et al. RXR-alpha ablation in skin keratinocytes results in alopecia and epidermal alterations. Development. 2001; 128:675–88. [PubMed: 11171393]

Li M, Indra AK, Warot X, Brocard J, Messaddeq N, Kato S, et al. Skin abnormalities generated by temporally controlled RXRalpha mutations in mouse epidermis. Nature. 2000; 407:633–6. [PubMed: 11034212]

Lippens S, Hoste E, Vandenabeele P, Agostinis P, Declercq W. Cell death in the skin. Apoptosis. 2009; 14:549–69. [PubMed: 19221876]

Lu YP, Lou YR, Yen P, Mitchell D, Huang MT, Conney AH. Time course for early adaptive responses to ultraviolet B light in the epidermis of SKH-1 mice. Cancer Res. 1999; 59:4591–602. [PubMed: 10493513]

Matsumura Y, Moodycliffe AM, Nghiem DX, Ullrich SE, Ananthaswamy HN. Resistance of CD1d−/− mice to ultraviolet-induced skin cancer is associated with increased apoptosis. Am J Pathol. 2004; 165:879–87. [PubMed: 15331412]

Metzger D, Indra AK, Li M, Chapellier B, Calleja C, Ghyselinck NB, et al. Targeted conditional somatic mutagenesis in the mouse: temporally-controlled knock out of retinoid receptors in epidermal keratinocytes. Methods Enzymol. 2003; 364:379–408. [PubMed: 14631857]

Mitchell DL, Nairn RS. The biology of the (6-4) photoproduct. Photochem Photobiol. 1989; 49:805–19. [PubMed: 2672059]

Murase D, Hachiya A, Amano Y, Ohuchi A, Kitahara T, Takema Y. The essential role of p53 in hyperpigmentation of the skin via regulation of paracrine melanogenic cytokine receptor signaling. J Biol Chem. 2009; 284:4343–53. [PubMed: 19098008]

Olivier M, Hussain SP, Caron de Fromentel C, Hainaut P, Harris CC. TP53 mutation spectra and load: a tool for generating hypotheses on the etiology of cancer. IARC Sci Publ. 2004:247–70. [PubMed: 15055300]

Noonan FP, et al. Neonatal sunburn and melanoma in mice. Nature. 2001; 413:271–272. [PubMed: 11565020]

Ouhtit A, Muller HK, Davis DW, Ullrich SE, McConkey D, Ananthaswamy HN. Temporal events in skin injury and the early adaptive responses in ultraviolet-irradiated mouse skin. Am J Pathol. 2000; 156:201–7. [PubMed: 10623668]

Proksch E, Brandner JM, Jensen JM. The skin: an indispensable barrier. Exp Dermatol. 2008

Quevedo WC Jr, Fleischmann RD. Developmental biology of mammalian melanocytes. J Invest Dermatol. 1980; 75:116–20. [PubMed: 6771335]

Rundhaug JE, Mikulec C, Pavone A, Fischer SM. A role for cyclooxygenase-2 in ultraviolet light-induced skin carcinogenesis. Mol Carcinog. 2007; 46:692–8. [PubMed: 17443745]

Saraiya M, Glanz K, Briss PA, Nichols P, White C, Das D, et al. Interventions to prevent skin cancer by reducing exposure to ultraviolet radiation: a systematic review. Am J Prev Med. 2004; 27:422–66. [PubMed: 15556744]

Sato T, Kawada A. Mitotic activity of hairless mouse epidermal melanocytes: its role in the increase of melanocytes during ultraviolet radiation. J Invest Dermatol. 1972; 58:392–5. [PubMed: 5030660]

Setlow RB, Swenson PA, Carrier WL. Thymine Dimers and Inhibition of DNA Synthesis by Ultraviolet Irradiation of Cells. Science. 1963; 142:1464–6. [PubMed: 14077026]

Shimizu H, Banno Y, Sumi N, Naganawa T, Kitajima Y, Nozawa Y. Activation of p38 mitogen-activated protein kinase and caspases in UVB-induced apoptosis of human keratinocyte HaCaT cells. J Invest Dermatol. 1999; 112:769–74. [PubMed: 10233770]

Slominski A, Paus R. Melanogenesis is coupled to murine anagen: toward new concepts for the role of melanocytes and the regulation of melanogenesis in hair growth. J Invest Dermatol. 1993; 101:90S–7S. [PubMed: 8326158]

Song X, Mosby N, Yang J, Xu A, Abdel-Malek Z, Kadekaro AL. alpha-MSH activates immediate defense responses to UV-induced oxidative stress in human melanocytes. Pigment Cell Melanoma Res. 2009; 22:809–18. [PubMed: 19659742]

Stierner U, Rosdahl I, Augustsson A, Kagedal B. UVB irradiation induces melanocyte increase in both exposed and shielded human skin. J Invest Dermatol. 1989; 92:561–4. [PubMed: 2703724]

Strom SS, Yamamura Y. Epidemiology of nonmelanoma skin cancer. Clin Plast Surg. 1997; 24:627–36. [PubMed: 9342506]

Sucov HM, Dyson E, Gumeringer CL, Price J, Chien KR, Evans RM. RXR alpha mutant mice establish a genetic basis for vitamin A signaling in heart morphogenesis. Genes Dev. 1994; 8:1007–18. [PubMed: 7926783]

Tripp CS, Blomme EA, Chinn KS, Hardy MM, LaCelle P, Pentland AP. Epidermal COX-2 induction following ultraviolet irradiation: suggested mechanism for the role of COX-2 inhibition in photoprotection. J Invest Dermatol. 2003; 121:853–61. [PubMed: 14632205]

van Schanke A, Jongsma MJ, Bisschop R, van Venrooij GM, Rebel H, de Gruijl FR. Single UVB overexposure stimulates melanocyte proliferation in murine skin, in contrast to fractionated or UVA-1 exposure. J Invest Dermatol. 2005; 124:241–7. [PubMed: 15654980]

Walker GJ, Kimlin MG, Hacker E, Ravishankar S, Muller HK, Beermann F, et al. Murine neonatal melanocytes exhibit a heightened proliferative response to ultraviolet radiation and migrate to the epidermal basal layer. J Invest Dermatol. 2009; 129:184–93. [PubMed: 18633434]

Werner S, Smola H. Paracrine regulation of keratinocyte proliferation and differentiation. Trends Cell Biol. 2001; 11:143–6. [PubMed: 11306276]

Whiteman DC, Whiteman CA, Green AC. Childhood sun exposure as a risk factor for melanoma: a systematic review of epidemiologic studies. Cancer Causes Control. 2001; 12:69–82. [PubMed: 11227927]

Wilgus TA, Parrett ML, Ross MS, Tober KL, Robertson FM, Oberyszyn TM. Inhibition of ultraviolet light B-induced cutaneous inflammation by a specific cyclooxygenase-2 inhibitor. Adv Exp Med Biol. 2002; 507:85–92. [PubMed: 12664569]

Wolnicka-Glubisz A, Noonan FP. Neonatal susceptibility to UV induced cutaneous malignant melanoma in a mouse model. Photochem Photobiol Sci. 2006; 5:254–60. [PubMed: 16465311]

Wulff BC, Schick JS, Thomas-Ahner JM, Kusewitt DF, Yarosh DB, Oberyszyn TM. Topical treatment with OGG1 enzyme affects UVB-induced skin carcinogenesis. Photochem Photobiol. 2008; 84:317–21. [PubMed: 18086242]

Yada Y, Higuchi K, Imokawa G. Effects of endothelins on signal transduction and proliferation in human melanocytes. J Biol Chem. 1991; 266:18352–7. [PubMed: 1917960]

Yasui H, Sakurai H. Chemiluminescent detection and imaging of reactive oxygen species in live mouse skin exposed to UVA. Biochem Biophys Res Commun. 2000; 269:131–6. [PubMed: 10694489]

Yoshida A, Kanno H, Watabe D, Akasaka T, Sawai T. The role of heparin-binding EGF-like growth factor and amphiregulin in the epidermal proliferation of psoriasis in cooperation with TNFalpha. Arch Dermatol Res. 2008; 300:37–45. [PubMed: 17960400]

Young AR. Cumulative effects of ultraviolet radiation on the skin: cancer and photoaging. Semin Dermatol. 1990; 9:25–31. [PubMed: 2203440]

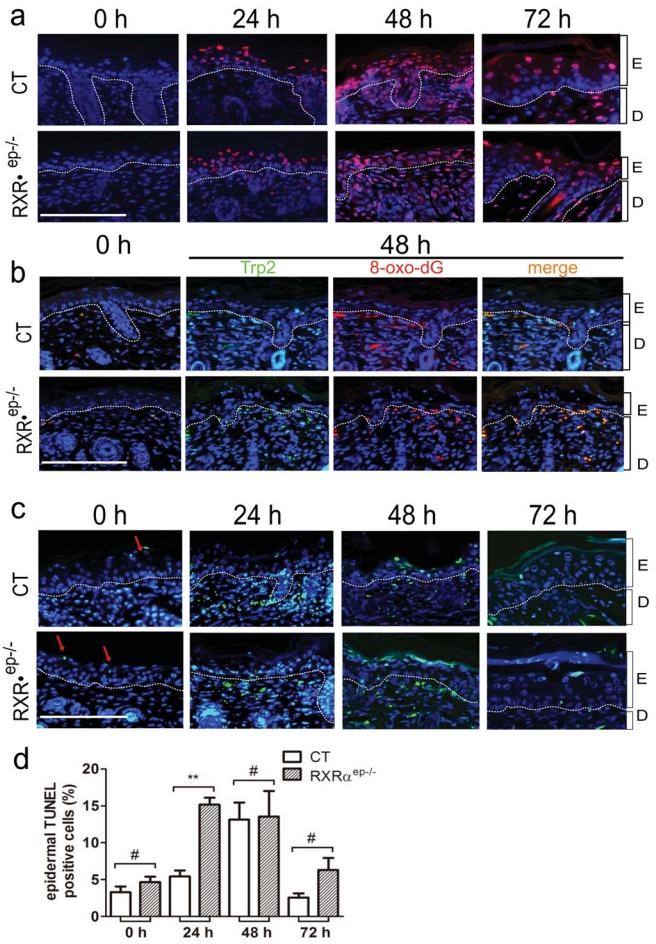

Figure 1. UVR induced DNA damage and apoptotic responses in control (CT) and RXRα$^{ep-/-}$ neonatal mice skin

(a) *Ex vivo* immunohistochemical analysis of DNA fragmentation in dorsal skin by detecting formation of thymine dimers (red). **(b)** Immunohistochemical detection of 8-oxo-dG (red) and TRP2 (green) positive cells in skin. Yellow color (merged panel) indicated Trp2^{+}/8-oxo-dG^{+} cells. **(c)**TUNEL assay for detection of apoptotic cells in non-irradiated and UV irradiated CT and RXRα$^{ep-/-}$ skin. Red arrows indicated TUNEL positive cells. **(d)** Percentage TUNEL+ (green) cells in CT and RXRα$^{ep-/-}$ mice epidermis before and after UVR. Percentage positive cells were counted as a percentage of total number of DAPI+ cells (blue) in epidermis. E=epidermis, D=dermis. Scale bar: 15.6 μm. Statistical analyses were performed by unpaired t-test; **, P<0.005; #=no statistical difference.

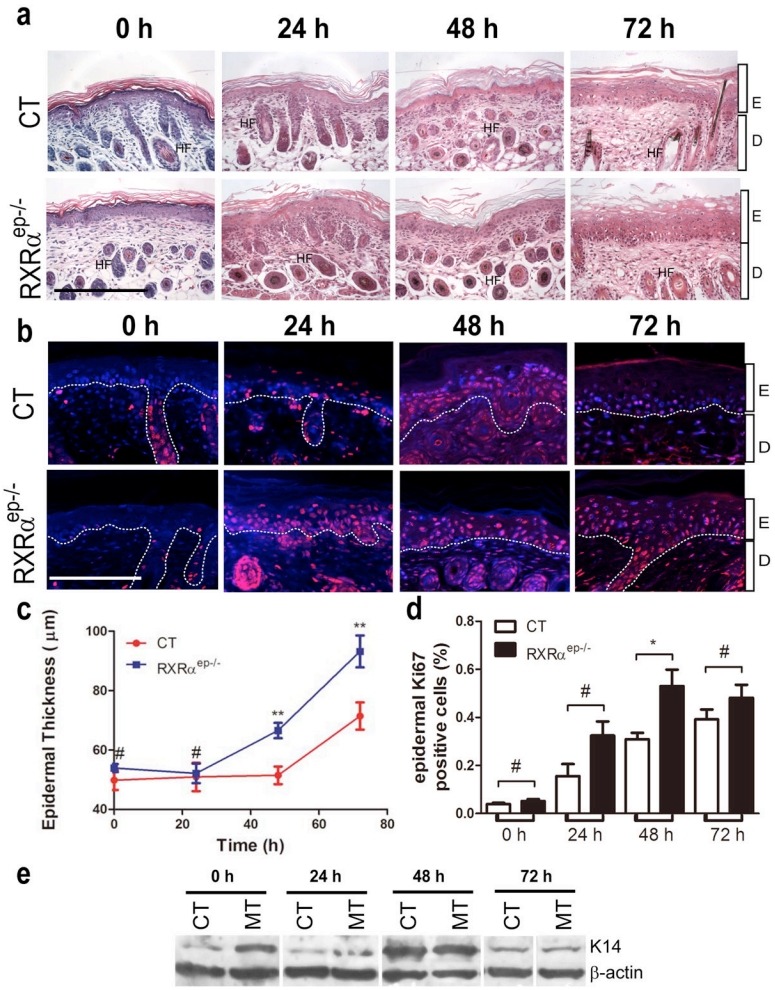

Figure 2. Enhanced Keratinocyte proliferative responses in CT and RXRα$^{ep-/-}$ mice upon UV stimulation

(a) Hemotoxylin-Eosin stained 5 μm thick paraffin sections from dorsal skin of neonatal CT and RXRα$^{ep-/-}$ mice. Scale bar: 31.2 μm**. (b)** Immunohistochemical staining with anti-Ki67 antibody (red). Scale bar: 15.6 μm. **(c)** Measurement of epidermal thickness in CT and RXRα$^{ep-/-}$ skin. **(d)** Percent Ki67-positive keratinocytes in CT and RXRα$^{ep-/-}$ skin. **(e)** Western blot analysis of K14 expression in CT and RXRα$^{ep-/-}$ mice before and after UV irradiation. β-actin was internal control. Separations between blots indicate lanes not originally run next to each other and juxtaposed in the figure. Sections were conterstained with DAPI (blue). Statistical analyses were performed by unpaired t-test and corrected with Bonferroni Step-down analysis; *, P<0.05; ** P< 0.005; #= no statistical difference. Hair follicles (HF), epidermis(E), dermis (D).

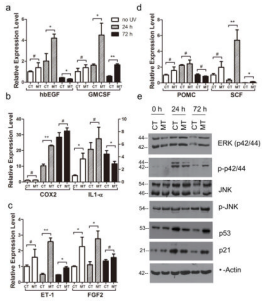

Figure 3. qRT-PCR analysis of expression of paracrine and autocrine factors, and western blot analysis of protein expression in skin of CT and RXRα$^{ep-/-}$ (MT) mice

Relative expression level of **(a)** hbEGF, GMCSF; **(b)** COX2, IL1-α, **(c)** ET-1, FGF2 and **(d)** POMC, SCF at different timepoints after UVR, as indicated. Values represent relative transcript level after normalization with HPRT transcripts. **(e)** Expression levels of different proteins such as ERK (p42/44), phospho-ERK, JNK, phospho-JNK, p53 and p21 were analyzed by western blot in control and mutant skin extracts obtained before and after UVR. β-actin was used as an internal control. Actual band sizes are indicated on the left of panel. *, P<0.2; ** P< 0.05; #=no statistical difference between CT and RXRα$^{ep-/-}$ mice.

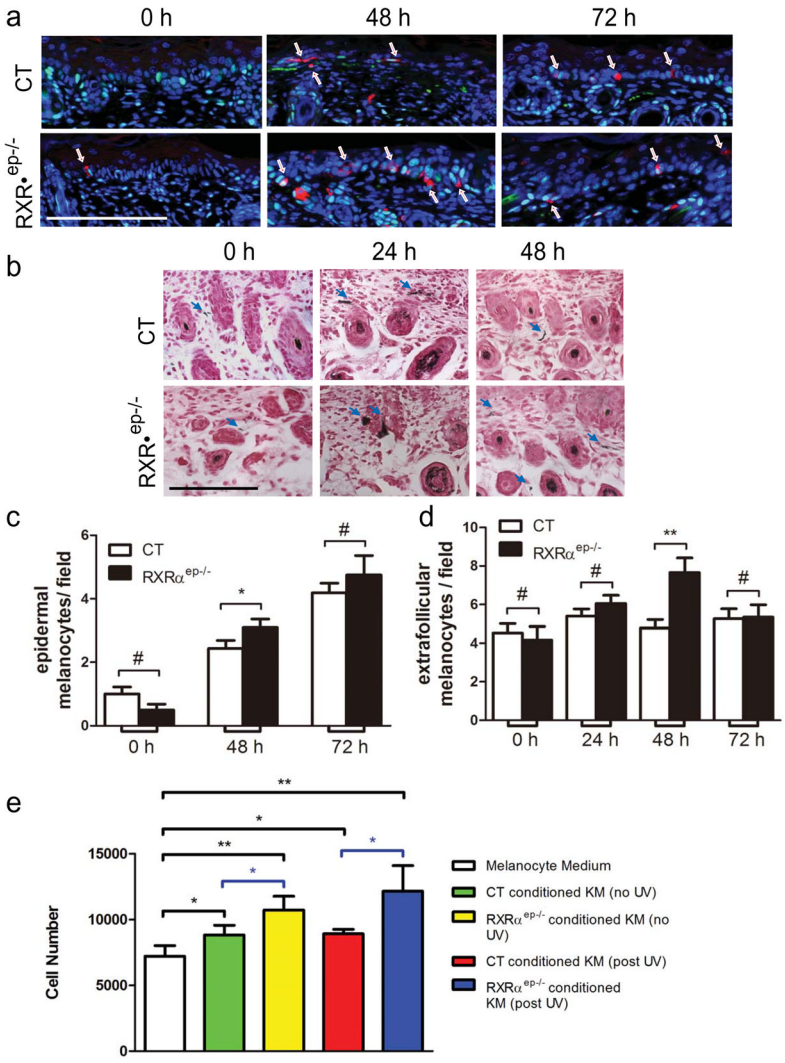

Figure 4. Effects of keratinocytic RXRα on melanocyte proliferation after UV exposure

(a) IHC staining for proliferating melanocytes with PCNA (green) and TRP1 (red). Nuclei were labeled with DAPI (blue). Arrows indicated epidermal melanocytes. **(b)** Fontana-Masson staining of control and RXRα$^{ep-/-}$ skin. Nuclei (pink-red), cytoplasm (pink) and melanin producing melanocytes (black) were indicated. Arrows indicated melanin producing melanocytes in dermis. Scale bar: 15.6 μm. Counting of melanocytes in CT and RXRa$^{ep-/-}$ **(c)** epidermis and **(d)** dermis at different timepoints. **(e)** Proliferation assay of primary melanocytes 24 hours after culture. Statistical analyses were performed by two-tailed unpaired t-test and corrected with Bonferroni Step-down analysis using GraphPad Prism software; *, P< 0.1; ** P< 0.05; #=no statistical difference. KM, keratinocyte medium.